Vector Control of Multiple Three-Phase Permanent Magnet Motor Drives

Sandro Rubino, Radu Bojoi
Dipartimento Energia "G. Ferraris"
Politecnico di Torino
Torino, 10129, ITALY

Emil Levi, Obrad Dordevic
Department of Electronics and Electrical Engineering
Liverpool John Moores University
Liverpool, L3 3AF, UNITED KINGDOM

***Abstract*—With the rapid development of power electronics, multiphase electrical solutions are becoming a competitive alternative to the conventional three-phase drives. Nowadays, the multiphase drives represent a robust and consolidated technology in both safety-critical and high-power applications. In addition, soon they will most likely be employed in the transportation electrification process. In this context, the multiple three-phase structures are undergoing an impressive development since they use the well consolidated three-phase technology reducing cost and design time. In this paper, a high-performance vector control for multiple three-phase permanent magnet motor drives is proposed. The developed solution employees a modular approach for the independent control of each three-phase unit. To show the feasibility of the developed control scheme, experimental results are provided for a nine-phase permanent magnet machine employing a triple three-phase configuration.**

Keywords—Multiphase electrical machines, permanent magnet motor drives, modular vector control

I. Introduction

In the recent years, an impressive electrification process has been started involving many production sectors. Among these ones, the transportation electrification is playing a leading role. However, this important technology change is requiring robust and reliable solutions able to replace the traditional ones. Thanks to the recent advancements of the power electronics, many electrical structures have been developed to satisfy this important need. In this context, the multiphase systems represent a smart and competitive solution [1-3].

Thanks to their fault tolerant behaviour, the multiphase electrical machines are a consolidated technology in marine propulsion and generation [4]. In addition, when the electric power levels approach the megawatts, the multiphase electrical machines are a natural solution for keeping the current level to acceptable limits that can be handled with today's fast power electronics components. In this way, it is possible to obtain high dynamic performance also in high power systems which are unthinkable of with the conventional thyristor technology.

Among all possible multiphase typologies, the multiple three-phase structures (Fig. 1) represent an interesting solution for the industrial manufacturers as the three-phase technologies have reached an impressive development together with a strong cost reduction. In this context, the multiple three-phase topology represents a convenient solution because the machine's stator consists of three-phase windings (with isolated neutral points) fed by independent three-phase converters [5-7]. In this way, the power converter can be structured in multiple three-phase power electronics

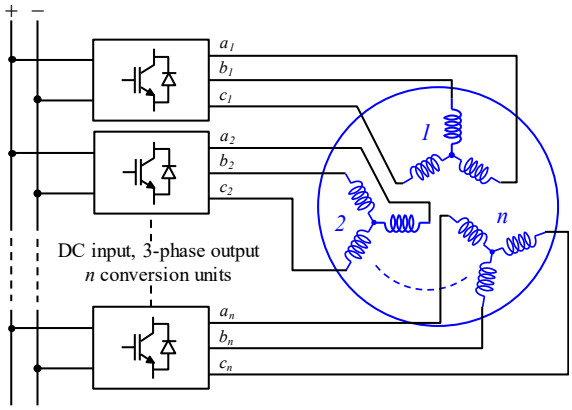

Fig. 1. Generic multiple three-phase drive topology.

modules with a relevant saving in terms of size, cost and development time [8]. In case of a power electronics fault, the faulted three-phase unit (winding plus converter) is simply disconnected from the dc power supply, thus yielding a straightforward post-fault reconfiguration.

In terms of machine manufacturing, the multiple three-phase structures require dedicated and expensive design methods to obtain the standard multiphase configurations (symmetrical/asymmetrical). In a cost-reduction scenario, a compromise solution is to use the existing off-the-shelf stator cores while potentially having to dispense with regular symmetrical/asymmetrical winding topologies. In this case, a modular structure is necessary not only from the drive topology point of view (Fig. 1), but also regarding the drive control scheme. For this reason, the goal of the work is to propose a modular vector control scheme for multiple three-phase permanent magnet motor drives. Following the current trend in the three-phase drives, the choice of a permanent magnet (PM) machine is a part of the induction motor replacement with PM machines due to better power density and efficiency [9].

The paper is organized as follows. Section II contains an exhaustive analysis of the modelling of multiple three-phase PM machines. The proposed control scheme is described in Section III while the test rig and experimental results are given in Section IV. Finally, Section V concludes the paper.

II. Modeling of Multiple Three-Phase PM Machines

The multiple three-phase machines can be modelled in many ways. However, the most frequently employed approach is the Vector Space Decomposition (VSD) one [10]. It allows configuring the machine model in multiple orthogonal bidimensional subspaces. Only one subspace is responsible for the electromechanical conversion, with similar equations to the conventional three-phase machines.

The other subspaces are considered as harmonic type and without any contribution in the torque production. Despite the simplicity, the VSD approach possesses two important limitations. The first one is the limited decoupling action only for regular asymmetrical and symmetrical multiphase configurations. The second one is the lack of modularity which prevents a viable design of drive control schemes, able to deal with direct and independent control of the individual three-phase sets (Fig. 1).

To solve these issues, the Multi-Stator (MS) approach is proposed in [4-5, 11]. The MS approach considers the machine as multiple three-phase units which run in parallel. For each three-phase unit, a dedicated three-phase Clarke transformation is applied. In this way, n overlapped three-phase stationary models are obtained, where n is the number of three-phase sets (Fig. 1). The MS approach can be applied for any multiple three-phase structure and it allows to preserve the mathematical modularity as each three-phase set is independently treated. More details about the MS approach for both induction and synchronous machines are reported in [4]. In synthesis, for each three-phase set the general three-phase Clarke transformation is applied:

$$[T_k] = \frac{2}{3} \cdot \begin{bmatrix} \cos(\vartheta_k) & \cos(\vartheta_k + 2\pi/3) & \cos(\vartheta_k + 4\pi/3) \\ \sin(\vartheta_k) & \sin(\vartheta_k + 2\pi/3) & \sin(\vartheta_k + 4\pi/3) \\ 1/2 & 1/2 & 1/2 \end{bmatrix} \quad (1)$$

where ϑ_k is the angle considered for the three-phase k-set; this angle is defined as the position of the first phase (a-phase) of the k-set with respect to the α-axis; the latter is conventionally made coincident with the first phase of the first set (a_1-phase).

A. Electromagnetic (d,q) Frame Model

According to [4], the application of the MS approach on a generic multiple three-phase PM machine leads to n stator complex electric and magnetic equations. For each k-set the stator electric model is computed as follows:

$$\bar{v}_{sk,dq} = R_{sk} \cdot \bar{i}_{sk,dq} + \frac{d}{dt}\bar{\lambda}_{sk,dq} + j \cdot \omega_r \cdot \bar{\lambda}_{sk,dq} \quad (2)$$

where $x_{sk,dq} = [x_{sk,d} \quad x_{sk,d}]^t$ is a generic stator vector defined for the three-phase k-set and referred to the physical (d,q) frame. The d-axis is conventionally defined as the N-pole direction of the magnets, as shown in Fig. 2 for a PM isotropic machine. To deal with the most generic case, in (2) different values of the stator resistances R_{sk} between the three-phase sets are assumed. The variables v_s, i_s and λ_s have the meaning of stator voltage, current, and flux, respectively. Finally, the variable j is the conventional complex vector operator. The electrical rotor position is denoted through the variable $\vartheta_r = p \cdot \vartheta_m$, where p is the pole pair number, while ϑ_m is the mechanical rotor position. The rotor electric speed is $\omega_r = p \cdot \omega_m$, where ω_m is the mechanical rotor speed.

The stator magnetic model for each k-set is defined as follows:

$$\bar{\lambda}_{sk,dq} = L_{lsk} \cdot \bar{i}_{sk,dq} + \begin{bmatrix} M_d & 0 \\ 0 & M_q \end{bmatrix} \cdot \sum_{z=1}^{n} \bar{i}_{sz,dq} + \begin{bmatrix} \lambda_m \\ 0 \end{bmatrix} \quad (3)$$

where L_{lsk} is the stator leakage inductance of the three-phase k-set, while M_d and M_q are the magnetizing inductances in d-axis and q-axis, respectively. The term λ_m represents the flux linkage amplitude of each k-set caused by the presence of the PM. It can be noted how the MS approach is able to manage different values of the stator parameters (R_{sk} - L_{lsk}) among the three-phase sets. This is another important limitation of the VSD approach, where identical stator parameters between the phases must be assumed.

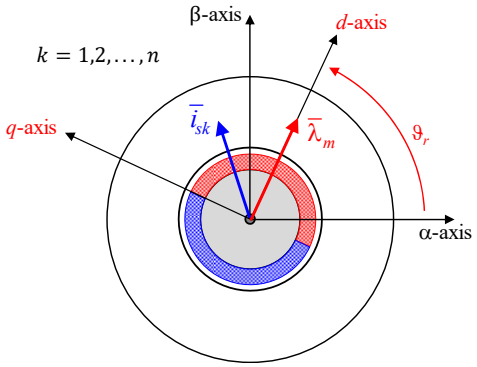

Fig. 2. (d,q) frame for a 2-pole multiple three-phase PM isotropic machine.

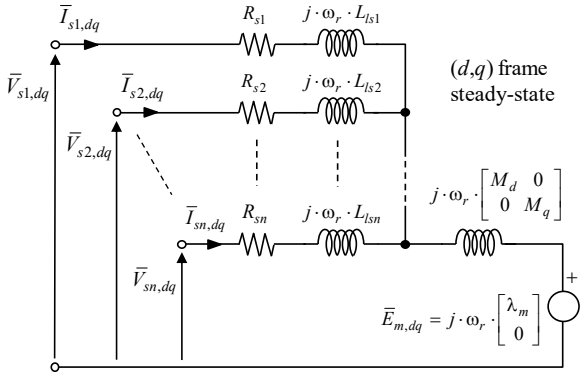

Fig. 3. Steady-state (d,q) MS model for a generic PM machine.

Finally, the PM machine electromagnetic torque T is given by (4) and represents the sum of n outer (vector) products:

$$T = \frac{3}{2} \cdot p \cdot \sum_{z=1}^{n} \left(\bar{\lambda}_{sz,dq} \wedge \bar{i}_{sz,dq} \right). \quad (4)$$

According to (2)-(4), the MS approach defines n different stator flux linkage vectors and current vectors and the total electromagnetic torque is the sum of the contributions of the n stator sets that interact with the rotor. Furthermore, the modularity of the MS approach is evident, as each three-phase set is characterized by its own electrical, magnetic and torque equations.

The steady-state (d,q) frame equivalent circuit of an IPM machine is shown in Fig. 3, where the individual contribution of each three-phase stator set can be noted. Lastly, when the machine is isotropic a unique value of the magnetizing (d,q) inductances can be employed:

$$M_d = M_q = L_m . \quad (5)$$

B. State-space Equations in (d,q) Frame

An important advantage of the VSD approach is the straightforward computation of the state equations. Indeed, the state-space equations of the main subspace are identical with the ones of the three-phase machines. Conversely, with the MS approach the computation of the state-space model is not easy since all the magnetic equations (3) are coupled.

To simplify the solutions and in accordance with the machine used for the experimental work, a PM isotropic structure (5) is considered. To make easier the interpretation of the state-space equations, the following auxiliary variables are defined:

$$c_z = L_m \cdot \frac{x_z}{L_{lsz}} \quad , \quad c_k = \sum_{\substack{z=1, \\ z \neq k}}^{n} c_z$$

$$R_{eq,k} = R_{sk} \cdot (1 + c_k) \quad , \quad L_{eq,k} = L_m + c_k \cdot L_{lsk} \qquad (6)$$

$$R_{eq,z} = c_z \cdot R_{eq,z}$$

where x_z is a logic value related to the state of the considered z-set (0-off/1-on). In this way, it is possible to reconfigure the state equations after an open-winding fault event. The computation of the state equations in the physical (d,q) frame for a single k-set (k=1,2…,n) leads to the following results:

$$L_{eq,k} \cdot \frac{d}{dt} \bar{i}_{sk,dq} = -\left(R_{eq,k} + j \cdot \omega_r \cdot L_{eq,k}\right) \cdot \bar{i}_{sk,dq} - j \cdot \omega_r \cdot \lambda_m + \\ + (1 + c_k) \cdot \bar{v}_{sk,dq} + \sum_{\substack{z=1 \\ z \neq k}}^{n} \left(R_{eq,z} \cdot \bar{i}_{sz,dq} - c_z \cdot \bar{v}_{sz,dq}\right). \qquad (7)$$

Equation (7) represents the electromagnetic dynamic model of a generic multiple three-phase PM isotropic machine. It can be noted how the dynamics of the currents in each set depend only partially on the k-set voltage. Indeed, due the use of the MS approach there are strong coupling effects between the sets. Both are reported under the summation operator in (7). The first coupling effect is in terms of current while the second one is in terms of voltage. The voltage couplings between the sets cannot be neglected because they can cause instability phenomena when a modular and independent current control of each unit is performed [7]. Therefore, in the drive scheme a decoupling action between the reference voltages must be included.

III. Modular Vector Control Scheme

The goal of this paper is to propose a high-performance modular vector control of a generic multiple three-phase PM machine implemented in the rotating rotor (d,q) frame. In this way, torque sharing operations do not imply any change in the rotational transformations since there is a total independence from the load angle value of each three-phase set.

The main advantage of a modular drive scheme is the possibility to obtain a direct control of the phase currents in each three-phase set independently of the employed multiphase configurations or/and eventual asymmetries between the stator parameters [4-5]. The drive control scheme is shown in Fig. 4. The torque reference is provided by an outer loop, in this case a speed regulator. However, it could be a dc voltage regulator if the machine is employed as a PM alternator.

The proposed drive scheme is structured in n current vector control modules which run in parallel. Each of them is dedicated to the current control of a single three-phase unit. Since the vector control is implemented in the rotating (d,q) frame, for each three-phase set, the (d,q) current values must be obtained. Therefore, by using the three-phase Clarke transformation defined in (1), the measured phase current values in the stationary (α,β) frame are firstly computed. The

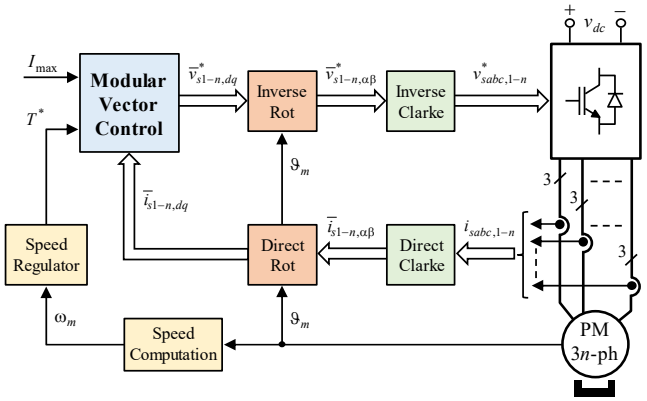

Fig. 4. Modular vector control of a multiple three-phase PM machine.

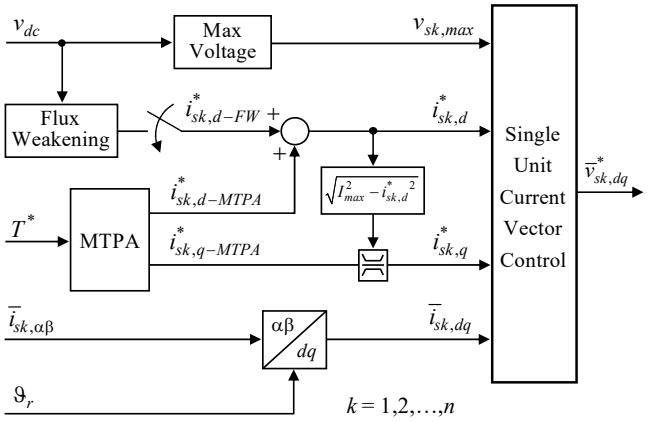

Fig. 5. Vector control scheme of a k^{th} set.

stationary values are then converted in the rotating (d,q) frame through the well-known rotational transformation, as shown in Figs. 4-5. The d-axis position ϑ_r is obtained through the measurement of the mechanical angle ϑ_m by means of an angular position sensor (usually a rotary encoder). The eventual mounting offset is compensated through the conventional self-commissioning procedures employed in the three-phase drive schemes.

According to the total torque reference T^*, the optimal (d,q) current values are computed. The simplest choice is to follow the Maximum-Torque-per-Ampere (MTPA) profile of the machine for the better exploitation of the power converter current range I_{max}, as shown in Fig. 5. By combining (3)-(5), the MTPA current values for an PM isotropic machine can be computed as follows:

$$i^*_{sk,d-MTPA} = 0 \quad , \quad i^*_{sk,q-MTPA} = \frac{T^*}{1.5 \cdot p \cdot n \cdot \lambda_m}. \qquad (8)$$

Expression (8) is defined under the hypothesis of magnetic linearity. Nevertheless, to improve the efficiency an accurate machine mapping can be performed [12]. In this case, the optimal MTPA current values are obtained by means of pre-loaded look-up tables.

The d-axis reference current $i^*_{sk,d}$ can be further modified if the Flux-Weakening (FW) operation is enabled, as shown in Fig. 5. In this case, the d-axis reference current is obtained as sum of the optimal MTPA value and the output of the FW regulator $i^*_{sk,d-FW}$ (usually a voltage regulator for each three-phase set [13]).

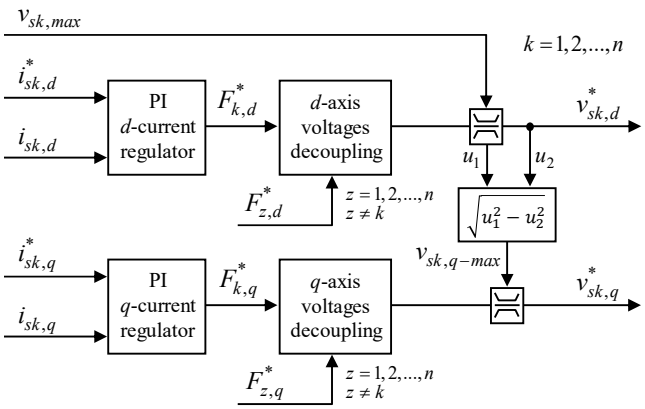

Fig. 6. Current vector control of a k^{th} set.

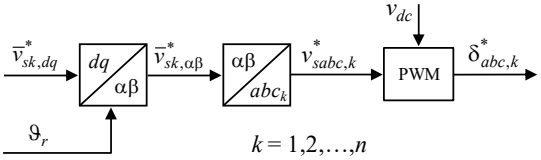

Fig. 7. Phase voltages reference computation of a k^{th} set.

Once the d-axis reference current has been obtained, the q-axis reference current $i^*_{sk,q}$ is eventually saturated to respect the maximum current limit I_{max}, as shown in Fig. 5. The machine used for the experimental validation has not been designed for FW operation as its characteristic current is much higher than the rated current. For this reason, the design and analysis of the FW regulator is beyond the scope of this paper.

Once the (d,q) reference currents are computed, the vector control is started. A pair of (d,q) current regulators is employed for each three-phase k-set, as shown in Fig. 6. Nevertheless, the outputs of the current regulators must not be considered as the (d,q) reference voltages for the considered k-set. Indeed, it is necessary to perform the voltage decoupling action described in Section II. According to (7), the outputs of the (d,q) current regulators correspond to the linear combinations of the voltage references belonging to all sets:

$$\begin{aligned} F^*_{k,d} &= (1+c_k)\cdot v^*_{sk,d} - \sum_{z=1,z\neq k}^{n}\left(c_z\cdot v^*_{sz,d}\right) \\ F^*_{k,q} &= (1+c_k)\cdot v^*_{sk,q} - \sum_{z=1,z\neq k}^{n}\left(c_z\cdot v^*_{sz,q}\right) \end{aligned} \quad . \tag{9}$$

Therefore, a decoupling action for each axis must be performed. After some mathematical manipulations, it is possible to demonstrate how the decoupling action is equivalent to applying the following solutions:

$$\begin{aligned} v^*_{sk,d} &= \left(1+\sum_{z=1}^{n}c_z\right)^{-1}\cdot\left[F^*_{k,d}+\sum_{z=1}^{n}\left(c_z\cdot F^*_{z,d}\right)\right] \\ v^*_{sk,q} &= \left(1+\sum_{z=1}^{n}c_z\right)^{-1}\cdot\left[F^*_{k,q}+\sum_{z=1}^{n}\left(c_z\cdot F^*_{z,q}\right)\right] \end{aligned} \quad . \tag{10}$$

The application of (10) allows to obtain the complete modularity between all sets also from the machine control point of view. Once the (d,q) voltage references have been computed, each q-axis voltage is eventually saturated to respect the maximum voltage limit $v_{sk,max}$, as shown in Fig. 6. This value corresponds to $v_{dc}/\sqrt{3}$ (v_{dc} is the dc-link voltage) since independent three-phase modulators are employed, one for each k-set. In this way, the well-known three-phase modulation techniques [14] can be implemented, as shown in Fig 7. This is another important advantage of the multiple three-phase structure as each three-phase winding does not share the neutral point with the other ones.

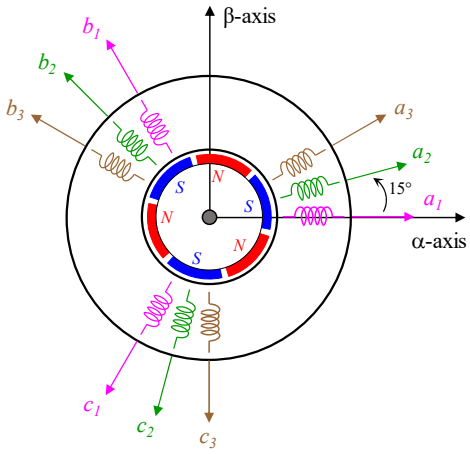

Fig. 8. 9-phase PM machine configuration (3x3ph, 6-pole).

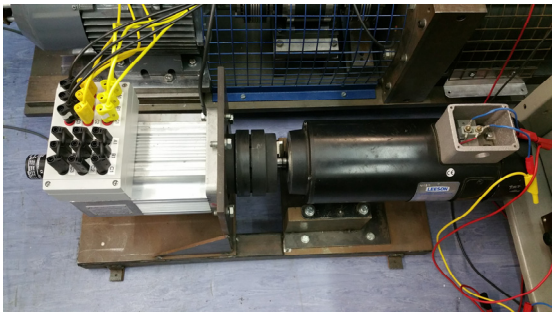

Fig. 9. View of the PM machine under test (left) and dc load machine (right).

IV. Experimental Validation

The proposed drive scheme has been validated on a nine-phase Surface Permanent Magnet machine (SPM) using a triple three-phase configuration. More specifically, the machine has been obtained starting from a three-phase prototype by rewinding the stator to reduce cost and design time. The original machine had 6-poles and 36 stator slots. Due the simultaneous high number of poles and stator phases, the total number of slots was not sufficient to build a conventional symmetrical/asymmetrical nine-phase configuration.

As a result, an unconventional machine configuration has been obtained with a relative shift of 15 electrical degrees between the three-phase sets instead of 20 electrical degrees (typical for the nine-phase asymmetrical configuration), as shown in Fig. 8. In addition, the second set (a_2,b_2,c_2) is characterized by different values of the stator parameters with respect to the other ones. Indeed, the equivalent electrical angular displacement between two stator slots is 30° electrical. Consequently, the second set has been obtained by splitting each phase winding between two consecutive slots.

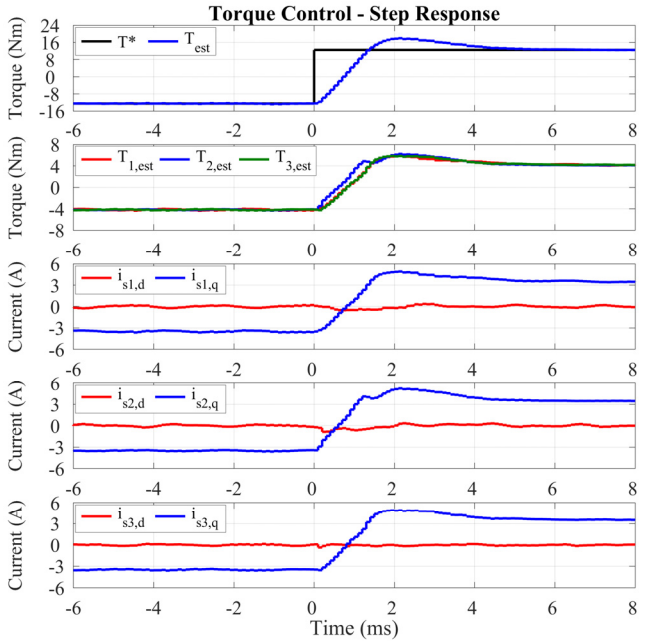

Fig. 10. Torque step response from 175% rated torque in generation to 175% rated torque in motoring at 1500 rpm. From top to bottom: reference and estimated total torque (Nm), estimated single sets torque (Nm), single sets measured (d,q) currents (A).

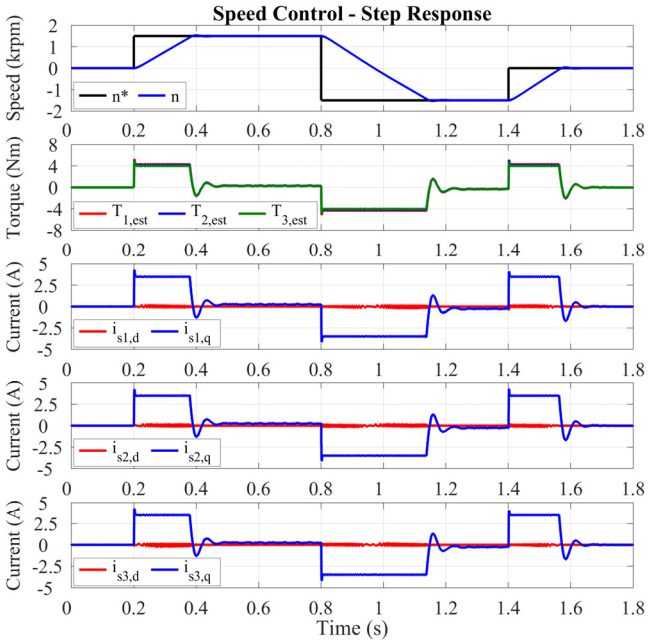

Fig. 11. Speed step response sequence (0 to 1500 rpm, 1500 rpm to -1500 rpm, -1500 rpm to 0 rpm) with inertial load. From top to bottom: reference and measured speed (krpm), estimated single sets torque (Nm), single sets measured (d,q) currents (A).

Therefore, despite the same number of winding turns the second set has a stator leakage inductance which is one half with respect to the other ones. Consequently, the VSD approach cannot be used, thus leading to replacement of the VSD with the MS that allows modularity. The machine's parameters are listed in Appendix.

The machine has been mounted on a test rig for validation purposes. The rotor shaft has been coupled to a dc machine acting as mechanical active load (Fig. 9). The power converter consists of two custom-made inverters, based on Infineon FS50R12KE3 IGBT modules fed by a single dc power source of 450V. The inverters have hardware-implemented dead time equal to 6 µs. The digital controller is the dSpace DS1106 development board. The switching frequency has been set at 5 kHz while the sampling frequency has been set to 10 kHz. A double-edge PWM modulation has been employed. The mechanical rotor position has been measured through a rotary incremental encoder. Due the mechanical limitations of the test rig, the maximum speed has been limited to ± 1500rpm. The experimental results are related to the drive operation in open loop torque control mode, followed by the ones in closed loop speed control mode.

The open loop torque control operations have been tested with the dc machine acting as prime mover (speed controlled). The speed has been set to 1500 rpm. The bandwidth of each current loop has been set to 600 Hz with a maximum allowable overshoot of 20% to demonstrate the high dynamic capability of the proposed drive scheme. The MTPA reference (d,q) currents for each three-phase set are computed by using (8).

The experimental results for a step torque transient from -12.5 Nm to + 12.5 Nm (175% of rated value) are shown in Fig. 10. The fast and well-controlled torque response can be noted, despite the inversion of the mechanical power from -2 kW to 2 kW in less than 2 ms. It is very interesting to note how the torque profile of the second set is characterised with rather faster dynamics than the other two. The reason is related to the lower value of the leakage inductance, which makes higher the current's derivative value, as demonstrated in (6)-(7).

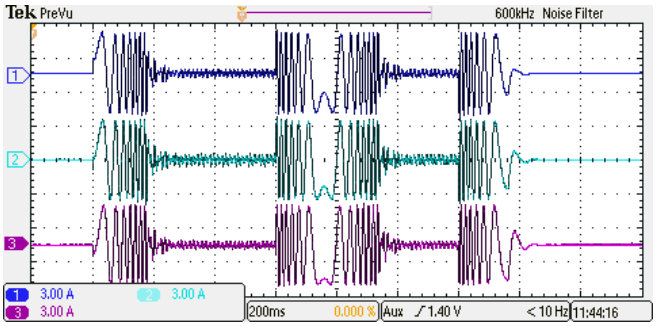

Fig. 12. Speed step response sequence (0 to 1500 rpm, 1500 rpm to -1500 rpm, -1500 rpm to 0 rpm) with inertial load. Ch1: $i_{sa,1}$ (3 A/div), Ch2: $i_{sa,2}$ (3 A/div), Ch3: $i_{sa,3}$ (3 A/div). Time resolution: 200 ms/div.

Despite this strong asymmetry, the modular vector control is perfectly able to manage each single set separately. Indeed, since the q-axis current of the second set reaches the reference value before the other two, it is possible to note a clamping action executed by the q-axis current loop of the second set in a completely independent way. This is the proof how a modular vector control scheme is perfectly able to deal with an independent control of each three-phase winding set.

The closed loop speed control operations have been tested with the dc machine acting as mechanical load (torque controlled). The bandwidth of the speed loop has been set to 20 Hz. The experimental results for a sequence of speed steps (0 rpm to 1500 rpm to -1500 rpm to 0 rpm) are shown in Figs. 11-12. It is possible to note the perfect speed response with an independent and balanced control of the torque produced by the single sets. To focus on the dynamics of the speed loop, the dc machine is off thus emulating a pure inertial load. Conversely, it has been controlled as passive and active load in the next test, related to the load response of the speed loop, as shown in Figs. 13-14.

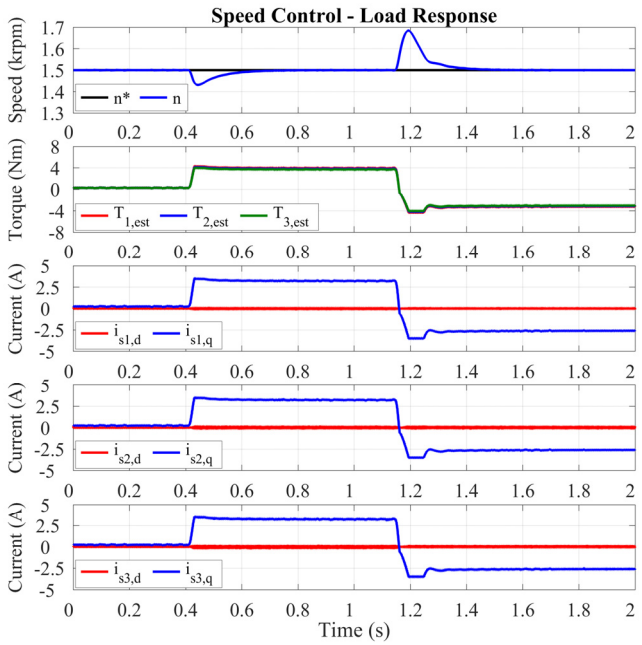

Fig. 13. Load response at 1500 rpm. From top to bottom: reference and measured speed (krpm), estimated single sets torque (Nm), single sets measured (*d*,*q*) currents (A).

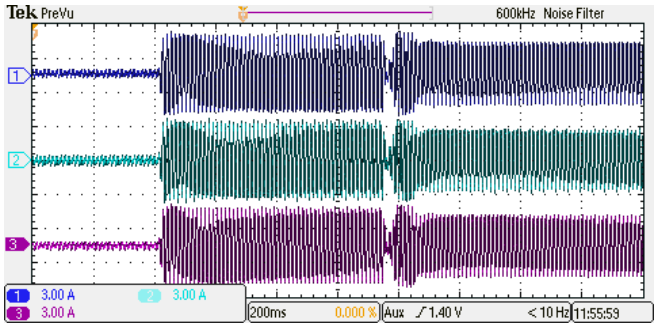

Fig. 14. Load response at 1500 rpm. Ch1: $i_{sa,1}$ (3 A/div), Ch2: $i_{sa,2}$ (3 A/div), Ch3: $i_{sa,3}$ (3 A/div). Time resolution: 200 ms/div.

In this test, an initial load step of +12 Nm is applied by the dc machine, so the speed loop immediately increases the torque demand to the three sets in modular way. The torque/current response of each set is well controlled, as shown in Fig. 13. Finally, the mechanical load applied by the dc machine is inverted from +12 Nm to -12 Nm thus switching the nine-phase PM machine operation from motoring mode to generation mode. The torque inversion happens in modular way among the three-phase sets without any problem so demonstrating the feasibility of the proposed solution in all possible conditions. It can be also noted how the maximum current limit has been met in each current loop (I_{max} = 3.5 A), as shown in Figs. 13-14. This condition corresponds to the maximum torque condition in the speed loop (12.5 Nm). Indeed, as soon as the machine control exits from this condition the speed's derivative suddenly changes making speed profile non-smooth.

V. Conclusion

The paper proposes a modular vector control scheme for multiple three-phase PM machines. The proposed control scheme yields the highest degree of modularity of the electric drive, which can be applied to unconventional multiple three-phase configurations (adopted for cost reasons) for which the VSD approach cannot be used. The performance of the proposed control has been validated with a nine-phase PM machine using a triple three-phase configuration. The experimental results demonstrate the feasibility of the developed drive solution in both motoring and generator operations.

Appendix

The machine parameters are reported in Table I.

TABLE I. PM Machine Parameters

Machine Data	Set 1	Set 2	Set 3
Pole pairs *p*	3		
Stator resistance R_{sk}	8.2 Ω	7.9 Ω	8.2 Ω
Stator leakage inductance L_{lsk}	18.5	10.3	18.5
Magnetizing inductance L_m	10.5 mH		
Permanent magnet flux linkage λ_m	0.265 Vs		
Rated rms current	1.5 A		
Overall mechanical inertia	0.0133 kg·m^2		

References

[1] E. Levi, "Multiphase Electric Machines for Variable-Speed Applications," *IEEE Trans. Ind. Elect.*, vol. 55, no. 5, pp. 1893-1909, 2008.

[2] F. Barrero and M. J. Duran, "Recent Advances in the Design, Modeling, and Control of Multiphase Machines—Part I," in *IEEE Trans. Ind. Elect.*, vol. 63, no. 1, pp. 449-458, Jan. 2016.

[3] M. J. Duran and F. Barrero, "Recent Advances in the Design, Modeling, and Control of Multiphase Machines—Part II," in *IEEE Trans. Ind. Elect.*, vol. 63, no. 1, pp. 459-468, Jan. 2016.

[4] R. Bojoi, S. Rubino, A. Tenconi and S. Vaschetto, "Multiphase Electrical Machines and Drives: A Viable Solution for Energy Generation and Transportation Electrification," in *Proc. Int. Conf. and Expo. on Electrical and Power Engineering (EPE)*, Iasi, Romania, pp. 632-639, 2016.

[5] S. Rubino, R. Bojoi, A. Cavagnino and S. Vaschetto, "Asymmetrical twelve-phase induction starter/generator for more electric engine in aircraft," in *Proc. IEEE Energy Conversion Congress and Exposition (ECCE)*, Milwaukee, WI, 2016, pp. 1-8.

[6] I. Zoric, M. Jones and E. Levi, "Arbitrary Power Sharing Among Three-Phase Winding Sets of Multiphase Machines," in *IEEE Trans. Ind. Elect.*, vol. 65, no. 2, pp. 1128-1139, Feb. 2018.

[7] Y. Hu, Z. Q. Zhu and M. Odavic, "Comparison of Two-Individual Current Control and Vector Space Decomposition Control for Dual Three-Phase PMSM," in *IEEE Trans. on Ind. Appl.*, vol. 53, no. 5, pp. 4483-4492, Sept.-Oct. 2017.

[8] W. Cao, B. C. Mecrow, G. J. Atkinson, J. W. Bennett and D. J. Atkinson, "Overview of Electric Motor Technologies Used for More Electric Aircraft (MEA)," in *IEEE Trans. Ind. Elect.*, vol. 59, no. 9, pp. 3523-3531, Sept. 2012.

[9] G. Pellegrino, A. Vagati, B. Boazzo and P. Guglielmi, "Comparison of Induction and PM Synchronous Motor Drives for EV Application Including Design Examples," in *IEEE Trans. Ind. Appl.*, vol. 48, no. 6, pp. 2322-2332, Nov.-Dec. 2012.

[10] Y. Zhao and T. A. Lipo, "Space vector PWM control of dual three-phase induction machine using vector space decomposition," *IEEE Trans. Ind. Appl.*, vol. 31, no. 5, pp. 1100-1109, 1995.

[11] R. H. Nelson and P. C. Krause, "Induction Machine Analysis for Arbitrary Displacement Between Multiple Winding Sets," *IEEE Trans. Power App. and Syst.*, vol. PAS-93, no. 3, pp. 841-848, 1974.

[12] E. Armando, R. I. Bojoi, P. Guglielmi, G. Pellegrino and M. Pastorelli, "Experimental Identification of the Magnetic Model of Synchronous Machines," in *IEEE Trans. Ind. Appl.*, vol. 49, no. 5, pp. 2116-2125, Sept.-Oct. 2013.

[13] Jang-Mok Kim and Seung-Ki Sul, "Speed control of interior permanent magnet synchronous motor drive for the flux weakening operation," in *IEEE Trans. Ind. Appl.*, vol. 33, no. 1, pp. 43-48, Jan/Feb 1997.

[14] D. G. Holmes and T. A. Lipo, "*Pulse Width Modulation for Power Converters: Principles and Practice*," Wiley-IEEE Press, 2003.